Environ Sci Pollut Res (2016) 23:21794–21804
DOI 10.1007/s11356-016-7362-1

RESEARCH ARTICLE

Changes in subcellular distribution and antioxidant compounds involved in Pb accumulation and detoxification in *Neyraudia reynaudiana*

Chuifan Zhou[1] · Meiying Huang[1] · Ying Li[1] · Jiewen Luo[1] · Li ping Cai[1]

Received: 1 February 2016 / Accepted: 1 August 2016 / Published online: 14 August 2016

Abstract The effects of increasing concentrations of lead (Pb) on Pb accumulation, subcellular distribution, ultrastructure, photosynthetic characteristics, antioxidative enzyme activity, malondialdehyde content, and phytochelatin contents were investigated in *Neyraudia reynaudiana* seedlings after a 21-day exposure. A Pb analysis at the subcellular level showed that the majority of Pb in the roots was associated with the cell wall fraction, followed by the soluble fraction. In contrast, the majority of the Pb in the leaves was located in the soluble fraction based on transmission electron microscopy and energy dispersive X-ray analyses. Furthermore, high Pb concentrations adversely affected *N. reynaudiana* cellular structure. The changes in enzyme activity suggested that the antioxidant system plays an important role in eliminating or alleviating Pb toxicity, both in the roots and leaves of *N. reynaudiana*. Additionally, the phytochelatin contents in the roots and leaves differed significantly between Pb-spiked treatments and control plants. Our results provide strong evidence that cell walls restrict Pb uptake into the protoplasm and establish an important protective barrier. Subsequent vacuolar compartmentalization in leaves could isolate Pb from other substances in the cell and minimize Pb toxicity in other organelles over time. These results also demonstrated that the levels of antioxidant enzymes and phytochelatin in leaves and roots are correlated with Pb toxicity. These detoxification mechanisms promote Pb tolerance in *N. reynaudiana*.

Keywords Lead · *Neyraudia reynaudiana* · Subcellular distribution · Ultrastructure · Antioxidative defense system · Phytochelatin

Responsible editor: Hailong Wang

Electronic supplementary material The online version of this article (doi:10.1007/s11356-016-7362-1) contains supplementary material, which is available to authorized users.

✉ Li ping Cai
fjclp@126.com

[1] College of Forestry, Fujian Agriculture and Forestry University, Co-innovation center for soil and water conservation in red soil region of the Cross-straits, Fuzhou 350002, China

Introduction

A large number of high-quality lead (Pb), zinc (Zn), and manganese (Mn) mines are distributed in the major heavy metal mining area in South China. Owing to outdated mining technology and poor long-term management, serious heavy metal pollution has occurred in the soil around mining areas; specifically, massive mining, wastewater discharge, and tailing accumulation have resulted in high levels of soil Pb (Cheng and Hu, 2010). As a consequence, the surrounding ecological environment is deteriorating and land has become barren. Pb pollution has become the main restrictive environmental factor with respect to vegetation restoration in Pb/Zn mining areas. Numerous studies have confirmed that Pb is one of the most highly toxic metals in the environment for plants, animals, and humans (Wang and Zhang. 2006; Zhou et al., 2014). In our previous studies on the soil characteristics of an abandoned rare earth ore mine, we found that *Neyraudia reynaudiana* is an excellent green plant for soil and water conservation, soil reinforcement, and as a windbreak in South China; it not only grows well in the abandoned rare earth ore mining area but also maintains a relatively high biomass. It shows high adaptability in the harsh environment of the abandoned rare earth mine area and is resistant to drought, poor soil, acid, heavy metal pollution, etc. It is characterized by a well-developed root system (with root lengths up to 300 cm), strong stems, tillering ability, rapid growth, and

high biomass (heights up to approximately 300 cm and diameter approximately 1 cm) and can adapt to a variety of harsh environments. These unique features make *N. reynaudiana* one of several plants that is able to grow in Pb/Zn mining areas. Furthermore, previous studies have shown that *N. reynaudiana* exhibits high Pb accumulation in metal-enriched soil, i.e., 345–773 mg/kg in its aboveground portion, which is close to the critical concentration standard for Pb in hyperaccumulator plants (1000 mg/kg), and its bioconcentration coefficient is 0.19–1.69. The transfer coefficient of *N. reynaudiana* is 3.1–21.2 (Dai and Ning 2008). Studies have indicated that Pb bioaccumulation in the aboveground portion of *N. reynaudiana* can reach 11,008 mg/kg by adding EDTA as a chelating agent, and this was 16.5 times greater than the levels observed in a control group (Dai and Ning 2008). Owing to these characteristics, *N. reynaudiana* is highly suitable for bioremediation to decrease Pb pollution in mining areas. However, the heavy metal tolerance mechanism of *N. reynaudiana* is not clear, and this limits the use of *N. reynaudiana* in phytoremediation applications to treat abandoned soils contaminated with heavy metals, such as Pb and Cd.

In general, the mechanisms of Pb tolerance and detoxification in plants can be divided into two categories: external exclusion and internal tolerance. External exclusion is the mechanism by which plants prevent Pb ions from entering cells to avoid accumulation at sensitive sites or pump excess Pb ions out of cells (Bibi and Hussain 2005; Sharma and Dubey 2005). In the internal tolerance mechanism, Pb in the cell is transformed into less toxic forms via the synthesis of organic ligands of Pb ions, such as cysteine, glutathione (GSH), phytochelatin, and metallothionein, to ease the toxic effects of Pb on the plant (Verma and Dubey, 2003; Pourrut et al. 2011). However, as exogenous Pb increases, Pb accumulation in the plant increases. Pb causes oxidative stress in plants via the production of large amounts of reactive oxygen species (ROS), such as $O_2^{\cdot-}$ and $OH^{\cdot}$, which seriously affect the function of plant membrane systems. When environmental conditions are optimal and plant metabolism functions efficiently, a dynamic equilibrium can be achieved between the generation and quenching of ROS. In plants, complex antioxidant systems typically limit active hydroxyl damage to cells; these systems include enzymes, such as superoxide dismutase (SOD), peroxidase (POD), catalase (CAT), as well as non-enzyme active oxygen scavengers, such as ascorbic acid, GSH, and phenolic compounds. Antioxidant enzymes are key factors in plant resistance to oxidative stress, which induces an increase in antioxidant enzyme activity and, consequently, resistance (Sharma and Dubey 2005). However, research has shown that when antioxidant enzyme activity is inhibited in cells, ROS become excessive and oxidative damage to membrane systems occurs. Furthermore, Pb can damage various organs and tissues of plants, as well as the ultrastructure of subcellular fractions, such as chloroplasts, mitochondria, nuclei, and cell wall membranes. This damage affects organelle functions and, ultimately, photosynthesis, respiration, protein synthesis, cell division, and other normal physiological functions (Huang et al. 1997; Salazar and Pignata, 2014), resulting in plant physiological and biochemical dysfunction and damage. Plant resistance to Pb occurs via two routes, i.e., exclusion and enrichment. The former refers to the discharge of Pb after it is already absorbed by plants or the blockage of Pb transportation within plants. The latter mainly refers to the promotion of non-bioactive, non-toxic forms of Pb, such as Pb bound to the cell wall, vacuolar Pb, or complexes with organic acids or proteins, such as GSH and phytochelatin (Wu et al. 2013). After absorption and transportation, Pb can exist in various cell structures and can form chemical bonds, limiting its movement in plants and reducing toxicity (Qiao et al. 2015).

Therefore, studies of physiological and biochemical indexes of *N. reynaudiana* under heavy metal stress, and particularly its Pb absorption properties, subcellular Pb distribution, antioxidant indexes, cell membrane integrity, membrane lipid peroxidation, phytochelatin content, and ultrastructural changes, will greatly improve the understanding of the heavy metal tolerance and stress responses in *N. reynaudiana*. The purpose of this study was to (1) determine the toxicity of Pb on *N. reynaudiana*, (2) characterize the absorption and transportation mechanisms of Pb in *N. reynaudiana*, and (3) identify the key mechanism mediating detoxification in *N. reynaudiana*. These results provide a basis for the phytoremediation of soil polluted by Pb.

Methods

Plant material and growth conditions

N. reynaudiana seed was collected from a mountain in FuZhou, Fujian province, China. After 30 days, healthy and equally sized shoots of *N. reynaudiana* were grown in 2.5-L pots for 1 week in distilled water to initiate new roots. Then, the seedlings were treated with 0, 25, 50, 100, or 200 μM Pb supplied as $Pb(NO_3)_2$ in Hoagland's solution for 21 days (corresponding to actual concentrations of 0, 20.6, 38.7, 72.3, or 145 μM Pb). To prevent the precipitation of Pb, the KH_2PO_4 concentration was adjusted to 0.025 mM (Gupta et al. 2010). The pH of the nutrient medium was adjusted to 5.5 using 0.1 M NaOH or 0.1 M HCl and was continuously aerated with an aquarium pump and renewed every third day during the experiment. Each treatment was replicated in four different vessels using a randomized block design in a light-proof glass container.

Lead content in plants

N. reynaudiana plants treated with 0, 25, 50, 100, or 200 μM Pb for 3, 7, 14, and 21 days were harvested to measure Pb accumulation. Roots of intact plants were washed with distilled water for a metal analysis and immersed in 20 mM Na-EDTA for 15–20 min to remove adsorbed Pb adhering to the root surface. Then, *N. reynaudiana* plants were dried at 105 °C and digested with an acid solution containing 13 M HNO_3 and 1 M $HClO_4$. For quality control, ten repeated measurements were carried out with a standard Pb solution provided by the Institute of Geophysical and Geochemical Exploration, China (Qiao et al. 2015). The Pb concentration was determined using an atomic absorption spectrophotometer (TAS-990: Pgeneral, China) after digestion with HNO_3 and $HClO_4$. The heavy metal estimates were checked using certified standard reference material (SRM 1547, peach leaves) obtained from the National Institute of Standards and Technology (Gaithersburg, MD, USA) (Zhou et al. 2015).

Subcellular distribution of Pb in *N. reynaudiana* roots and leaves

N. reynaudiana plants treated with 0, 25, or 200 μM Pb for 3, 7, 14, and 21 days were harvested to measure the Pb subcellular fractions in leaves and roots, respectively. Subcellular fractions were isolated as described by Li et al. (2016). Frozen plants (0.5000 g) were homogenized using a chilled mortar and a pestle with 20 mL of pre-chilled extraction buffer (containing 50 mM Tris–HCl (pH 7.5), 250 mM sucrose, and 1.0 mM dithioerythritol). The homogenate was transferred to a 50-mL centrifuge tube and centrifuged at 300×*g* for 10 min at 4 °C. The pellet was considered the cell wall fraction (F1). The filtrate was centrifuged at 2000×*g* for 10 min, and the pellet was the nucleus-rich fraction (F2). The supernatant was then centrifuged at 10,000×*g* for 30 min. The pellet was designated the mitochondrial fraction (F3) and the supernatant was the soluble fraction (F4). All homogenizations and subsequent fractionations were performed at 4 °C (Nishizono et al. 1987). Pb concentrations in the fractions were determined by atomic absorption spectrophotometry using atomic absorption spectrometry (TAS-990, Pgeneral) after digestion with HNO_3 and $HClO_4$.

Transmission electron microscopy and energy dispersive X-ray analysis

N. reynaudiana plants treated with 0, 25, and 200 μM Pb for 21 days were selected for transmission electron microscopy (TEM). Small sections (1–3 mm long) from the middle of the third leaf from the top of the plant were fixed in 4 % glutaraldehyde (*v*/*v*) in 0.2 M sodium phosphate buffer (pH 7.2) for 6–8 h and post-fixed in 1 % OsO_4 for 1 h and in 0.2 M sodium phosphate buffer for 1–2 h. Dehydration was performed in a graded ethanol series (50, 70, 85, 90, and 95 %) followed by acetone, and then samples were infiltrated and embedded in Spurr's resin (Basile et al. 1994). Ultra-thin sections (80 nm) were prepared and mounted on copper grids for viewing using a transmission electron microscope (Tecnai G2 Spirit) at an accelerating voltage of 60.0 kV. Subsequently, the energy spectra of the prepared sections were measured using the JEM-2100 transmission electron microscope equipped with the Oxford IE250 Energy Dispersive Spectroscopy system (EDS; Abingdon, UK). The acceleration voltage was 150 kV, the removal angle was 25°, and the measurement time was 60 s. A qualitative elemental analysis was conducted with the electron beam fixed in the high electron density area of the sample (Basile et al. 1994).

Photosynthetic characteristics

Total chlorophyll content and the Chl *a* and Chl *b* contents from young shoots were estimated after extraction using 80 % methanol following previously described methods (Lichtenthaler and Buschmann 2001).

Determination of antioxidative enzyme activity and MDA content

Prior to biochemical analyses, wet leaf and root samples were homogenized with an extraction buffer containing 100 mM potassium phosphate buffer (pH 7.0), 0.5 % TritonX-100, and 1 % polyvinylpyrrolidone using a pre-chilled mortar and pestle (Zhou et al. 2013). The homogenate was centrifuged at 15,000×*g* for 20 min at 4 °C. The supernatant obtained after centrifugation was used to determine SOD, CAT, and POD activity. SOD activity was assayed using the xanthine–xanthine oxidase and nitroblue tetrazolium system. One unit of SOD was defined as the amount of protein that inhibited the rate of nitroblue tetrazolium reduction by 50 % (Zhou et al. 2014). The POD reaction solution contained 50 mM phosphate buffer (pH 7.8), 25 mM guaiacol, 200 mM H_2O_2, and the enzyme extract. Changes in the absorbance of the reaction solution were determined at 470 nm (Li et al. 2012). CAT activity was assayed immediately after centrifugation of the homogenates according to previously described methods (Aebi 1984). One unit of enzyme was defined as the amount necessary to decompose 1 mmol H_2O_2 min^{-1} at 25 °C. Lipid peroxidation (as MDA) was estimated according to previously established methods (Islam et al. 2008). Four milliliters of 0.5 % *tert*-butyl alcohol in 20 % trichloroacetic acid was added to a 1-mL aliquot of the supernatant, and the mixture was incubated in boiling water for 30 min. The MDA content was then determined spectrophotometrically at 532 nm and corrected for nonspecific turbidity at 600 nm.

Measurements of non-protein sulfhydryl, glutathione, and phytochelatin concentrations

Non-protein sulfhydryl (NPSH), GSH, and phytochelatin concentrations were determined in acidified leaf and root extracts prepared as described by De Vos et al. (1992). The NPSH content was measured spectrophotometrically with Ellman's reagent (5,5′-dithiobis-2-nitrobenzoicacid, DTNB). The supernatant (300 μL) was mixed with 630 μL of 0.5 M K_2HPO_4 solution, and absorbance at 412 nm was measured after 2 min. Two minutes after the addition of 26.6 μL of DTNB solution (6 mM DTNB, 0.143 M K_2HPO_4, 6.3 mM DTPA, pH 7.5), absorbance was measured again at 412 nm (Zhou et al. 2015). Reduced GSH was estimated according to previously described methods (Andersen et al. 1997). Phosphate buffer (60 μL, 100 mM, pH 7.0) and 40 μL of DTNB were added to 500 μL of the supernatant, and absorbance was read at 412 nm after 2 min. Total NPSH, GSH, and individual phytochelatin species concentrations are expressed as micromole SH per gram fresh weight. Total phytochelatin concentrations (μmol) were estimated by subtracting GSH from NPSH (Zhou et al. 2015).

Statistical analysis

All statistical analyses were implemented in SPSS 19.0 for Windows (SPSS Inc., Chicago, IL, USA). Values are reported as the means of four replicates, except for TEM and EDS data. One-way ANOVA was applied to assess the differences between groups, and significant differences ($p < 0.05$) were then evaluated by post hoc SNK multiple range tests; statistical significance was assessed at $\alpha = 0.05$.

Results

Effects of Pb on plant growth and photosynthesis

N. reynaudiana was exposed to solutions with various concentrations of Pb for 21 days. Compared with the control, when the Pb concentration was greater than 100 μM, the growth of the underground portion of *N. reynaudiana* was significantly inhibited ($p < 0.05$). When the Pb concentration was greater than 200 μM, the growth of the aboveground portion of *N. reynaudiana* was significantly inhibited ($p < 0.05$). These results indicated that as the Pb concentration in the solution increased slightly, the growth of the root system of *N. reynaudiana*, but not the aboveground portion, was initially inhibited. However, as the concentration of Pb continued to increase, the inhibition of aboveground growth was detected (Fig. S1). However, chloroplast pigments (Chl *a*, Chl *b*, and total Chl) did not differ significantly between the treatments and the control (Fig. S2).

Pb accumulation in the roots and shoots of *N. reynaudiana* at various time points

Based on water culture experiments (Fig. 1a), the Pb contents in the roots and the aboveground portions of *N. reynaudiana* increased significantly as the Pb concentration in the treatment solution increased. After 21 days, the Pb contents in roots increased significantly from 0 to 577.9, 1157.8, 4053.2, and 5349.2 mg kg^{-1} for increasing Pb concentrations (Fig. 1a), while those in the leaves increased from 0 to 85.3, 98.2, 180.3, and 222.5 mg kg^{-1} (Fig. 1b). Different from the aboveground part, as the treatment time and Pb concentration increased, the amount of Pb absorbed by roots continued to increase and Pb contents were far higher than those observed in the aboveground plant parts (Fig. 1).

Subcellular distribution of Pb in roots and leaves for different exposure times

To study the subcellular distribution of Pb in different parts of *N. reynaudiana* and changes in the distribution over time, we

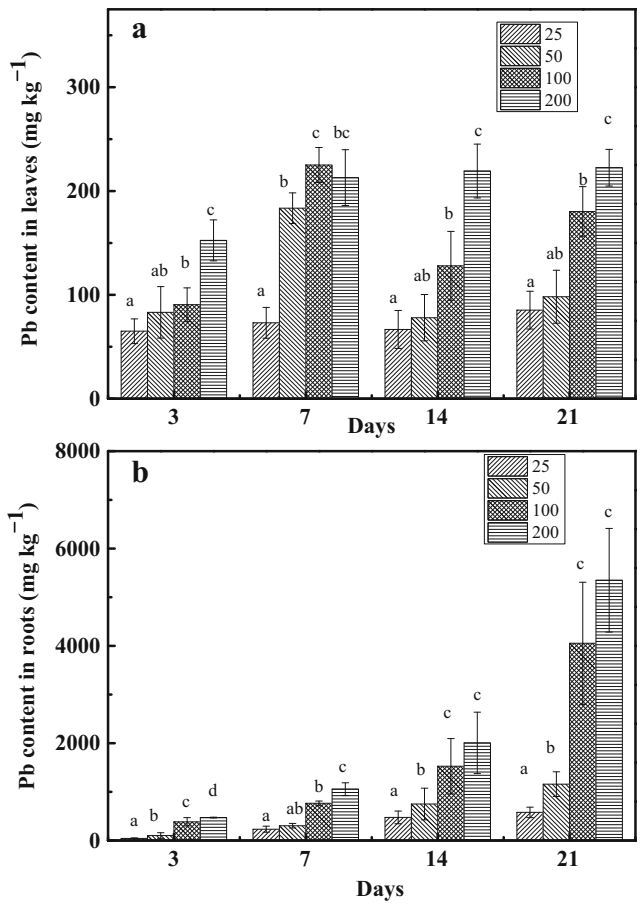

Fig. 1 Accumulation of Pb in *N. reynaudiana* after a 21-day exposure to the Pb-spiked solution. *Bars* represent means ± S.E. of four independent replicates. Pb was not detected in the 0-μM Pb group. *Bars that do not share the same letters* are significantly different at $P < 0.05$, as determined by SNK multiple range tests

compared two treatment groups, i.e., a low Pb concentration of 25 μM and a high Pb concentration of 200 μM. At 25 μM Pb, the overall Pb contents in the subcellular structures of the aboveground parts of *N. reynaudiana* were as follows (in decreasing order): F4 (soluble component), F3 (mitochondria), F2 (nuclei and chloroplasts), F1 (cell wall) (Fig. 2). At 25 μM Pb, there was little variation in Pb contents in each subcellular structure over time. At 200 μM Pb, the Pb contents in the subcellular structure of the aboveground parts of *N. reynaudiana* showed the following pattern (in decreasing order): F4 > F3 > F1 > F2. In the leaves, Pb was primarily distributed in the soluble components of F4. As exposure time increased, Pb contents in each component did not change significantly. In root cells, the overall pattern of Pb in organelles was as follows: F1 > F2 > F4 > F3; these results indicated that root Pb was primarily distributed in the cell wall. As exposure time increased, Pb contents in organelles continued to increase and the relative Pb contents in different organelles changed. Specifically, the relative Pb content in F1 decreased, while the proportion of Pb in F4 increased, suggesting that the treatments reduced the retention effect of cell walls on Pb, while the compartmentalization effect of the soluble fraction on Pb increased.

Transmission electron microscopy and energy dispersive X-ray analysis

The effects of stress on the subcellular structure of various organs and tissues of *N. reynaudiana* were visualized directly using TEM (Figs. 3 and 4). Based on TEM observations of *N. reynaudiana* root cells in the blank control group, root-tip cells were structurally normal; the cell wall showed smooth and continuous characteristics and the endoplasmic reticulum and plasmodesmata were clearly visible (Fig. 3a, b). Additionally, the toxic effects of 25 and 200 μM Pb treatments on the subcellular structures of the root-tip tissues could be directly visualized (Fig. 3c–f); in particular, the cell wall color deepened, possibly reflecting an increase in brittleness, resulting in fracturing or roughening in some areas. At the break points of the plasmodesmata, loose materials at the edge of the cell wall were visible, and they drifted toward the cell cavity. Additionally, some Pb particles were deposited in the vicinity of the inner cell wall. However, the damage to membrane structures attached to the cell walls was more serious. Compared with cells shown in Fig. 3a, b, the cells shown in Fig. 3c–f had a large amount of black materials deposited at the inside and outside of the cell wall. These black materials were insoluble compounds containing Pb based on an energy spectrum analysis (Fig. S3). The cell wall deposits differed among location, wherein the deposits in root cell walls were dots or granular in structure, while the deposits in the center of the root cells were granular.

Based on observations of the leaf structure (Fig. 4a–c), the cell plasma membrane and the cell wall were closely connected in the plant leaves in the control group. The double layers of the nuclear membrane were clearly visible with prominent nucleoli. The chloroplast membranes were complete; the grana thylakoids were tightly stacked with numerous layers; and the cavities of the grana thylakoids were small and flat, were arranged parallel to the long axis in the same direction, and were connected with the stroma thylakoids to form a continuous membrane system. The mitochondrial morphology was normal. Chloroplasts in the control group were oval with distinct structures. The double-layer membranes were complete. The grana and stroma lamella were arranged neatly and contained starch grains and osmiophilic granules, and they

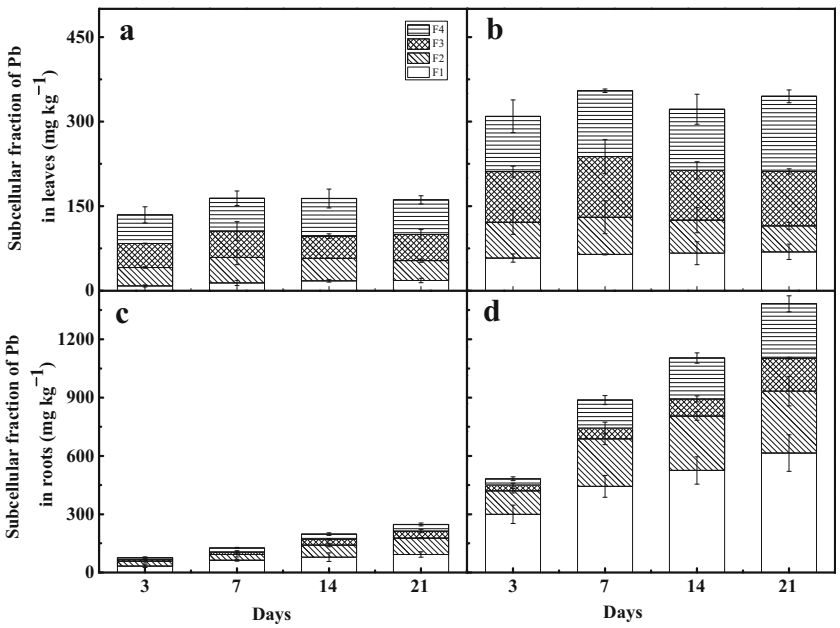

Fig. 2 Subcellular distribution of Pb in roots and leaves of *N. reynaudiana* for different Pb treatments and exposure times (**a**, **b** 25 μM Pb treatment; **c**, **d** 200 μM Pb treatment). *Bars* represent means ± SE of four independent replicates

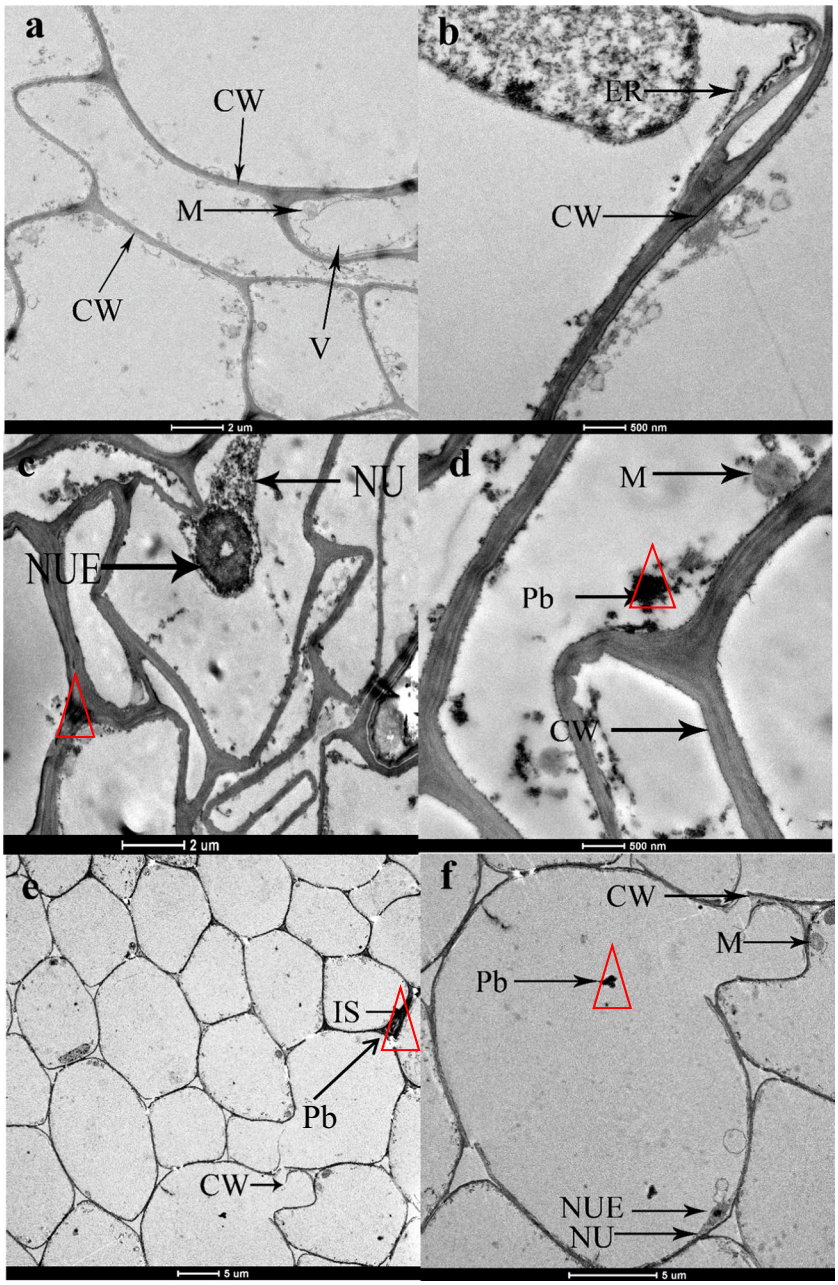

Fig. 3 Ultrastructure of *N. reynaudiana* root cells for different Pb treatments (**a**, **b** *N. reynaudiana* exposed to 0 μM Pb for 21 days; **c**, **d** *N. reynaudiana* exposed to 25 μM Pb for 21 days; **e**, **f** represent *N. reynaudiana* exposed to 200 μM Pb for 21 days). Labels: *CW* cell wall, *IS* intercellular space, *M* mitochondrion. *N* nucleus, *NUE* nucleolus, *OP* osmiophilic particles, *V* vacuoles. Images were obtained using a JEM-2100 transmission electron microscope

were arranged along the cell edge to facilitate light absorption and the rapid transportation of photosynthetic products. However, Pb stress significantly changed the cell structure in *N. reynaudiana* leaf cells (Fig. 4d–h). After Pb stress, the common features observed included a damaged chloroplast, a decreased ratio of the long axis to the short axis, and in some cases, expansion into a spherical shape. The high-concentration Pb treatment resulted in significant damage to parts of the chloroplasts, which showed incomplete structures. The double-layer membranes were broken or the structures disappeared, the internal grana lamella were disordered, and the remaining grana and stroma thylakoids were loose and exhibited increased swelling. Owing to the uneven expansion, the grana appeared wavy and were in a dissociative state.

After treatments with 25 and 200 μM Pb, large amounts of black materials were deposited at the cell walls, cell gaps, and inside cell walls in the roots and leaves of *N. reynaudiana* (Fig. 3c, d). These deposits were granular. Based on EDS analysis (Fig. S3), the black deposits had similar element compositions, i.e., mainly Pb, C, O, and Si. The areas with black spots contained Pb, and a denser distribution of black spots and greater particle number were associated with more Pb deposition in the area. Therefore, the cell walls, cell gaps, and vacuoles were the main sites of Pb accumulation in the

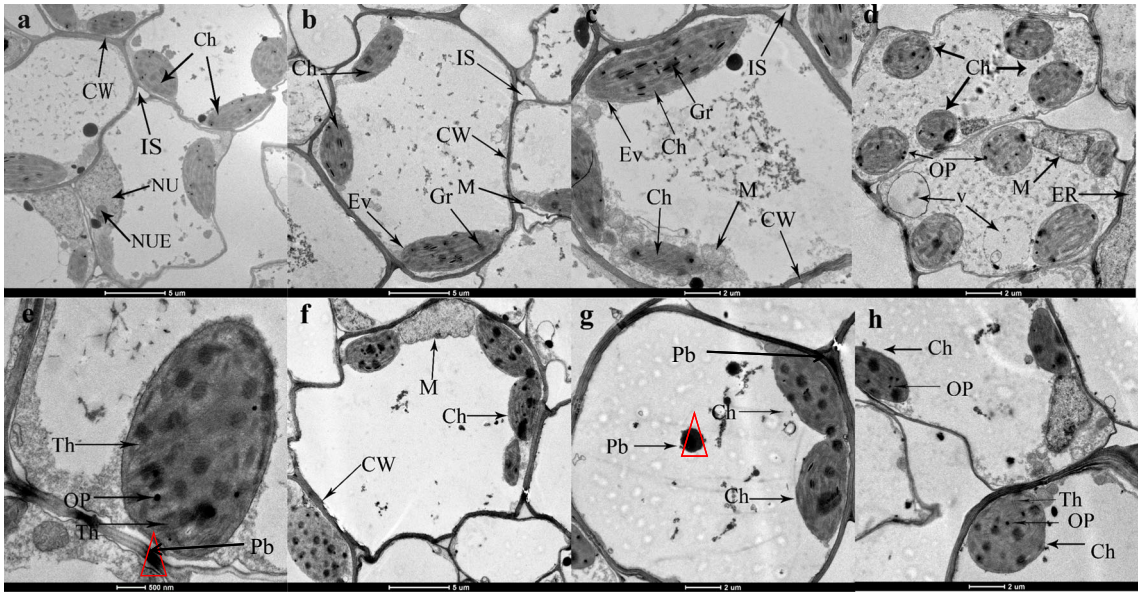

Fig. 4 Ultrastructure of leaf cells of *N. reynaudiana* plants exposed to different Pb treatments for 21 days (**a**–**c** the results for *N. reynaudiana* exposed to 0 μM Pb for 21 days; **d**, **e** *N. reynaudiana* exposed to 25 μM Pb for 21 days; **f**–**h** *N. reynaudiana* exposed to 200 μM Pb for 21 days). Labels: *Ch* chloroplast, *CW* cell wall; *Gr* granum grain, *IS* intercellular space, *M* mitochondrion. *N* nucleus, *NUE* nucleolus, *OP* osmiophilic particles, *Th* thylakoid, *V* vacuoles. Images were obtained with a JEM-2100 transmission electron microscope

roots and leaves of *N. reynaudiana*, which is consistent with the results shown in Fig. 2.

Effects of Pb on antioxidant enzyme activity and MDA content

Compared with the control group, 21 days after exposure to the Pb solution, SOD, CAT, and POD activity in the leaves and the root system of *N. reynaudiana* increased significantly ($p < 0.05$) (Fig. 5a–c), and the SOD, CAT, and POD contents in the roots were higher than those in the leaves. These results suggest that Pb stress promoted an oxidative stress reaction in the roots and leaves of *N. reynaudiana*, and the roots showed a stronger antioxidant capacity. In addition, exposure to Pb resulted in a significant increase in malondialdehyde (MDA) in a dose-dependent manner in the roots and the leaves. Collectively, these results indicate that Pb exposure resulted in cell membrane damage and lipid peroxidation in roots and leaves (Fig. 5d).

Effect of Pb on non-protein sulfhydryls, glutathione, and phytochelatins

Under Pb stress, the overall changes in the GSH content in the roots and leaves of *N. reynaudiana* were not significant, but the changes in non-protein thiols (NPSH) and phytochelatin were significant. NPSH and phytochelatin contents in the roots of *N. reynaudiana* increased initially as the Pb concentration increased, but then gradually decreased. In the leaves, NPSH and phytochelatin contents increased significantly as the Pb concentration increased ($p < 0.01$), indicating that phytochelatin in the leaves of *N. reynaudiana* plays an important role in the process of detoxification (Fig. 6).

Discussion

Many studies have shown that in a hydroponic system, Pb concentrations exceeding 0.5 μM inhibit the growth of plants (Patra et al. 1994). In our experiment, *N. reynaudiana* showed no phenotypic abnormalities for all Pb treatments compared with the control plants, except for a Pb concentration of greater than 100 μM, for which root growth was inhibited. This indicated that *N. reynaudiana* had very strong Pb resistance, as well as very high capacity to cope with drastic changes in the external environment via a series of stress responses. Pb accumulation in *N. reynaudiana* under hydroponic conditions was greater in roots than in leaves, which was similar to the patterns found in studies of other hyperaccumulator plants, such as *Lepidium sativum* L. (Gill et al. 2012), *Eichhornia crassipes* (Srinivasan et al. 2014), and *Sedum alfredii* (Huang et al., 2012). The Pb concentration in the roots of *N. reynaudiana* increased significantly as the Pb concentration in solution increased, and showed an obvious dose–response relationship. This could indicate a protective measure initiated by *N. reynaudiana*, i.e., by detaining Pb in the roots, Pb transport to aboveground parts was limited, thus reducing Pb-induced interference and damage to photosynthesis in plant leaves and other important physiological and biochemical processes (Fig. 2) (Mingorance et al. 2012). Therefore, we

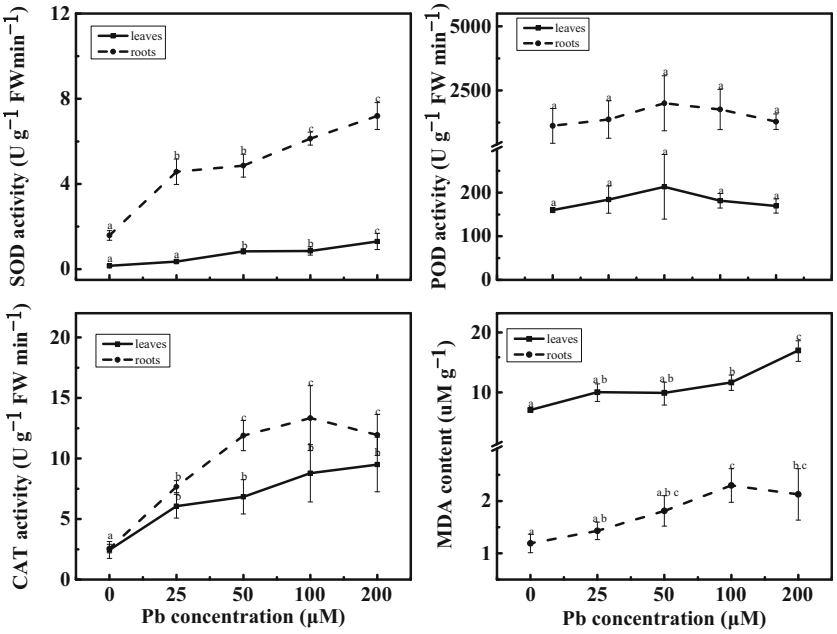

Fig. 5 Activities of superoxide dismutase (SOD) (**a**), peroxidase (POD) (**b**), and catalase (CAT) (**c**), and MDA content (**d**) in the leaves and roots of *N. reynaudiana* after a 21-day exposure to 0, 25, 50, 100, and 200 μM Pb in solution. Values are expressed as means ± SE of three independent replicates. Those not sharing the *same letters* are significantly different at $P < 0.05$ as determined by SNK multiple-range tests

speculated that two main mechanisms may be involved in obstructing Pb transportation to aboveground plant parts: (1) the endodermis Casparian strips in the roots blocked further Pb transport and (2) endothelial cells of the root tissue played a role in lateral retention, which blocked transportation of Pb to the aboveground parts (Sharma and Dubey 2005; Kopittke et al. 2008).

The subcellular distribution and accumulation mechanisms determine the tolerance of plants to Pb and their detoxification ability (Islam et al. 2008). We found that Pb accumulation in the subcellular structures of *N. reynaudiana* increased as the Pb concentration increased. In roots, the majority of Pb was distributed in the cell wall. TEM analyses confirmed that Pb particles existed in the cell walls. Previous studies have indicated that Pb sediment in the form of particles is structurally stable and is often difficult to transport aboveground (Islam et al. 2008). These sediments were likely phosphate precipitates, such as $Pb_5(PO_4)_3OH$, $Pb_3(PO_4)_2$, $Pb(H_2PO_4)_2$, and $Pb_5(PO_4)_3Cl$ (Islam et al. 2008; Kopittke et al. 2008). The cell wall distribution of Pb in *N. reynaudiana* could be explained as follows: (1) Pb^{2+} ions are positively charged and accordingly are easily adsorbed and deposited in large quantities in the negatively charged cell wall (Verma and Dubey, 2003) and (2) plant cell walls contain proteins and polysaccharides, such as cellulose, hemicellulose, and lignin, as well as a large number of coordinating groups, such as hydroxyl, carboxyl, aldehyde groups, and amino acids that easily adsorb Pb^{2+} ions (Islam et al. 2008; Pourrut et al. 2011). The non-protoplast parts of the cells, mainly the cell wall, have low physiological and metabolic activities and, as "dead tissues," are the first barrier to the entry of heavy metals in plant cells (Wu et al. 2013). Thus, reduced metal ion transport across the membrane and a decreased plasma concentration of metal ions may be associated with the distribution of Pb in tissues that lack metabolic activity, and this could mitigate or avoid damage to functional structural units of cells, i.e., protoplasts, as well as the disruption of metabolic processes. These results were consistent with those of previous studies (Liu et al. 2015; Qiao

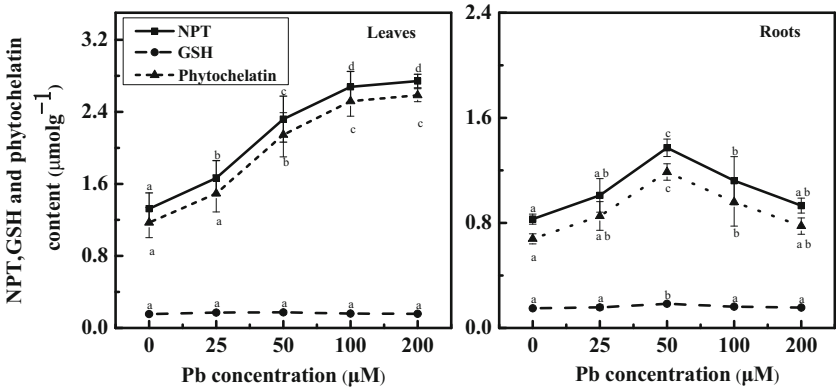

Fig. 6 Contents of non-protein sulfhydryl (NPSH), glutathione (GSH), and phytochelatins in **a** leaves and **b** roots of *N. reynaudiana* after a 21-day exposure to different concentrations of Pb. *Bars* represent means ± SE of three independent replicates. *Bars that do not share the same letters* are significantly different at $P < 0.05$ as determined by SNK multiple-range tests

et al., 2015). In addition, in a study of the subcellular distribution of Cd in the tissues of *Phytolacca americana* L., Fu et al. (2011) found that Cd was mainly distributed in the cell wall. In our previous studies, we found that at a low concentration, nearly 100 % of Pb is blocked by cell walls in the root system of *Conyza canadensis*, and Pb does not enter protoplasts. However, Islam et al. (2008) studied the toxic effect of Pb on two ecotypes of *Elsholtzia argyi* in mining and the non-mining areas by TEM and found that cell walls are the main sites of Pb accumulation in the roots of both ecotypes. Kopittke et al. (2008) found that Pb initially accumulates in the cytoplasm of the epidermal and cortical cells of *Brachiaria decumbens* and is eventually transferred to the cell wall and precipitated in the form of $Pb_5(PO_4)_3Cl$. Using synchrotron radiation X-ray absorption spectroscopy techniques, Tian et al. (2010) found that cell wall-bound Pb is the primary form of Pb in the hyperaccumulator ecotype *S. alfredii* Hance. As the primary subcellular fraction for Pb storage, Pb binding to cell walls is both an effective and important mechanism for Pb detoxification in *N. arundinacea*. A larger portion of Pb in the cell walls contributed to lower Pb accumulation in organelles and solution fractions, implying a higher capacity for biological Pb detoxification in *N. arundinacea*. However, this cell wall interception function had some limitations. For example, as the Pb exposure concentration increased, the Pb content in cell walls increased. Although the interception function of the cell wall still played an important role, the relative Pb content in the cell wall was significantly reduced (Fig. 2c, d). This might be explained by the saturation of heavy metals bound to the root cell wall. Alternatively, the increased toxic effects may result in damage to normal metabolic functions of *N. reynaudiana* cells, resulting in increased permeability of cell walls and plasma membranes and increased oxidative stress (Fig. 5); thereby, increased Pb may severely damage the interception capability of root cell walls (Sharma and Dubey 2005). A large number of Pb ions were allowed to enter the cell, which was confirmed by TEM and energy spectrum analyses (Fig. 4c–f). Additionally, as time increased, the proportion of Pb in the soluble components of F4 increased, indicating that most of the heavy metal ions that entered the cells were transported to and stored in the vacuoles for compartmentalization and to reduce Pb damage to other organelles. This reduces damage to chlorophyll or maintains its synthesis (Fig. S2), thereby enhancing plant resistance to heavy metals. In total, 6.0–20.1 and 31.2–41.3 % of total Pb was found in the soluble fraction including cell vacuoles in the shoots and roots of *N. arundinacea*, respectively. Plant vacuoles are principally composed of sulfur-rich peptides and organic acids, which can reduce toxicity via the complexation of metal with organic ligands. The sequestration of heavy metals in vacuoles could further prevent metal ions from interfering with organelle function (Zhao et al. 2015). Approximately 91 % of Zn in the protoplast is stored in the vacuoles of *Thlaspi caerulescens* leaves, which indicates that vacuoles are involved in metal tolerance (Ma et al. 2005). In addition, 72 % of Ni is distributed in the vacuoles of the hyperaccumulator *Alyssum serpyllifolium*. Wu et al. (2013) showed that vacuoles are the second major sites of Pb accumulation in *Brassica chinensis*, after the cell wall, based on differential centrifugation and synchrotron radiation X-ray fluorescence spectroscopy; the Pb contents in the vacuoles of the roots and aboveground tissues were as high as 26.9 and 38.0 %, respectively. This suggests that Pb sequestration in vacuoles could further reduce Pb toxicity in the cytoplasm and minimize Pb buildup in organelle fractions in *N. arundinacea*. However, our results indicated that Pb was localized in plant cell organelles under higher Pb stress, consistent with the results of Małecka et al. (2008). Accordingly, increased tolerance of *N. arundinacea* to Pb might be attributed to cell wall deposition and vacuolar compartmentalization, which minimize Pb accumulation in the organelle fraction and protect organelles from the negative effects of Pb (Patra et al. 1994).

Under normal conditions, active oxygen metabolism in plants is in a balanced state (Kosobrukhov et al. 2004; Bibi and Hussain 2005). Heavy metals react as lipid peroxidation-inducing agents and disrupt the balance between the production of free radicals and their clearance in cells, resulting in the production of large amounts of ROS and free radicals, such as $O_2^{\cdot-}$, $OH^{\cdot}$, NO, $RO^{\cdot}$, $ROO^{\cdot}$, H_2O_2, and ROOH (Sytar et al. 2013). This can lead to the denaturation of proteins and biomacromolecules and intensify cell membrane lipid peroxidation (Islam et al. 2008). The high level of ROS in plants could be a signal that triggers oxidative stress and programmed cell death. However, plants also have antioxidant protective enzymes, such as SOD, POD, and CAT, which are able to maintain a dynamic equilibrium between the production and removal of free radicals. Generally, it is thought that maintaining and improving the activities of SOD, POD, and CAT are important for plant tolerance to heavy metals (Sytar et al. 2013). We detected significant increases in the activities of SOD, POD, and CAT in the roots and leaves of *N. reynaudiana*. The increase in SOD enzymatic activity in *N. reynaudiana* resulted in $O_2^{\cdot-}$ removal. The activities of POD and CAT increased gradually to remove H_2O_2, which was generated by SOD dismutation and was further converted into non-toxic H_2O and O_2 to mitigate cell damage. This indicates that SOD, POD, and CAT played key roles in *N. reynaudiana* tolerance to Pb stress. Similar heavy metal detoxification mechanisms have been observed in *L. sativum* L. (Gill et al. 2012), *E. crassipes* (Srinivasan et al. 2014), and *S. alfredii* (Huang et al. 2012). MDA is a lipid peroxidation product of the biomembrane system, and it can react with the free amino group in proteins, resulting in intramolecular and intermolecular cross-linking and cell damage. MDA content plays an important role as an indicator of peroxidation

intensity and the extent of the membrane system damage. Generally, it is believed that cell membrane permeability increases with increasing concentrations of Pb. The plant cell membrane system is the material exchange interface between the plant and the environment, and its stability is the basis for normal physiological functions of cells (Sharma and Dubey 2005; Islam et al. 2008; Mingorance et al. 2012; Sytar et al. 2013). We found that under Pb stress, the MDA content in roots was significantly higher than that of the control group because Pb entered the cells (Fig. 2) and excessive oxygen free radicals accumulated, leading to lipid peroxidation. These results indicated that the regulatory capacity of antioxidation enzymes in roots was limited; the excess free radicals attacked unsaturated fatty acids on the cell membrane, weakening the cell membrane structure, and the permeability of the root cell membranes increased, which increases extravasation (Sytar et al. 2013).

S is an essential nutrient for animals and plants. Inorganic sulfur absorbed by plants can be converted into a variety of SH-containing compounds, such as GSH, phytochelatin, and thioredoxin, which play important roles in plant heavy metal tolerance. In particular, phytochelatin are SH-containing peptides composed of cysteine, glutamic acid, and glycine; they are induced by heavy metals in plants and play dual roles in resistance to heavy metal pollution. They not only chelate heavy metal ions but also function as important antioxidants. The H_2O_2 clearance abilities of phytochelatin are usually four to five times higher than those of GSH and AsA (Mishra et al. 2006). In our study, compared with the control group, the phytochelatin levels in the leaves and roots of *N. reynaudiana* were significantly higher. These results indicate that under Pb stress, *N. reynaudiana* can synthesize more phytochelatin in order to reduce Pb toxicity (Fig. 6). The formation of phytochelatin–metal complexes in response to Pb is well documented. Estrella-Gómez et al. (2009) found that the accumulation of phytochelatin in *Salvinia minima* is a direct response to Pb accumulation. The synthesis of NPSH and phytochelatin in the roots of the mining ecotype *Athyrium wardii* is significantly enhanced in response to Pb stress (Zhao et al. 2015). In addition, we found that phytochelatin formed complexes with Pb^{2+} in the cytoplasm, thus reducing Pb^{2+} toxicity in the metabolically active cellular compartment. Subsequently, such complexes were transferred to the vacuole and vacuolar compartmentalization was achieved (Figs. 3f and 4g showed extensive Pb depositions in vacuoles). These phytochelatin–Pb complexes that migrate into vacuoles might contribute to the compartmentalization and increased Pb concentration in the soluble fraction of tissues. The presence of phytochelatin–Pb complexes has been shown in vivo in various taxa, e.g., *S. minima* (Estrella-Gómez et al. 2009), *Vetiver grasses* (Andra et al. 2010), *Melilotus officinalis*, and *Melilotus alba* (Wu et al. 2013), suggesting their role in Pb tolerance.

Conclusions

Our results demonstrated that *N. reynaudiana* has strong Pb tolerance and a high Pb accumulation capacity. A high percentage of Pb was bound to the cell wall fraction and soluble fraction at the subcellular level in *N. reynaudiana*. Furthermore, *N. reynaudiana* increased phytochelatin compound synthesis to avoid Pb buildup in the organelle fraction under Pb stress. These characteristics indicated that cell wall deposition and vacuolar compartmentalization might be important Pb detoxification mechanisms in *N. reynaudiana*. Moreover, *N. reynaudiana* exhibited strong Pb resistance via its antioxidant capacity and phytochelatin synthesis to reduce Pb damage. These properties enabled it to grow in extremely Pb-polluted habitats and make it a good candidate for phytostabilization.

Acknowledgments This work was supported by the National Key Technology Support Program (2014BAD15B02), Foundation for Cultivation Plan of Distinguished Young Scholars of Fujian Province (2005), National Natural Science Foundation of China (31400465, 41401364), National Natural Science Foundation of Fujian (2013J01073).

References

Aebi H, (1984):Catalase in vitro. In: Lester, P. (Ed.). Methods in enzymology. Academic Press, pp. 121–126

Andersen HR, Nielsen JB, Nielsen F, Grandjean P (1997) Antioxidative enzyme activities in human erythrocytes. Clin Chem 43:562–568

Andra SS, Datta R, Sarkar D, Makris KC, Mullens CP, Sahi SV, Bach SB (2010) Synthesis of phytochelatins in vetiver grass upon lead exposure in the presence of phosphorus. Plant Soil 326:171–185

Basile A, Giordano S, Cafiero G, Spagnuolo V, Castaldo-Cobianchi R (1994) Tissue and cell localization of experimentally-supplied lead in *Funaria hygrometrica Hedw.* Using X-ray SEM and TEM microanalysis. J Bryol 18:69–81

Bibi M, Hussain M (2005) Effect of copper and lead on photosynthesis and plant pigments in black gram [*Vigna mungo (L.) Hepper*]. B Environ Contam Tox 74:1126–1133

Cheng H, Hu Y (2010) Lead (Pb) isotopic fingerprinting and its applications in lead pollution studies in China: a review. Environ Pollut 158:1134–1146

Dai W, Ning P (2008) Tolerance and accumulation of *Neyraudia reynaudiana* for Pb. Chinese Journal Of Environmental Engineering 2:1004–1008

De Vos CR, Vonk MJ, Vooijs R, Schat H (1992) Glutathione depletion due to copper-induced phytochelatin synthesis causes oxidative stress in *Silene cucubalus*. Plant Physiol 98:853–858

Estrella-Gómez N, Mendoza-Cózatl D, Moreno-Sánchez R, González-Mendoza D, Zapata-Pérez O, Martínez-Hernández A, Santamaría JM (2009) The Pb-hyperaccumulator aquatic fern *Salvinia minima* Baker, responds to Pb^{2+} by increasing phytochelatins via changes in SmPCS expression and in phytochelatin synthase activity. Aquat Toxicol 91:320–328

Fu X, Dou C, Chen Y, Chen X, Shi J, Yu M, Xu J (2011) Subcellular distribution and chemical forms of cadmium in *Phytolacca americana L.* J Hazard Mater 186:103–107

Gill SS, Khan NA, Tuteja N (2012) Cadmium at high dose perturbs growth, photosynthesis and nitrogen metabolism while at low dose it up regulates sulfur assimilation and antioxidant machinery in garden cress (*Lepidium sativum* L.). Plant Sci 182:112–120

Gupta DK, Huang HG, Yang XE, Razafindrabe BHN, Inouhe M (2010) The detoxification of lead in *Sedum alfredii* H. is not related to phytochelatins but the glutathione. J Hazard Mater 177:437–444

Huang JW, Chen J, Berti WR, Cunningham SD (1997) Phytoremediation of lead-contaminated soils: role of synthetic chelates in lead phytoextraction. Environ Sci Technol 31:800–805

Huang H, Gupta DK, Tian S, Yang X, Li T (2012) Lead tolerance and physiological adaptation mechanism in roots of accumulating and non-accumulating ecotypes of *Sedum alfredii*. Environ Sci Pollut R 19:1640–1651

Islam E, Liu D, Li T, Yang X, Jin X, Mahmood Q, Tian S, Li J (2008) Effect of Pb toxicity on leaf growth, physiology and ultrastructure in the two ecotypes of *Elsholtzia argyi*. J Hazard Mater 154:914–926

Kopittke PM, Asher CJ, Blamey FPC, Auchterlonie GJ, Guo YN, Menzies NW (2008) Localization and chemical speciation of Pb in roots of signal grass (*Brachiaria decumbens*) and Rhodes grass (*Chloris gayana*). Environ Sci Technol 42:4595–4599

Kosobrukhov A, Knyazeva I, Mudrik V (2004) *Plantago major* plants responses to increase content of lead in soil: growth and photosynthesis. Plant Growth Regul 42:145–151

Li X, Zhang L, Li Y, Ma L, Bu N, Ma C (2012) Changes in photosynthesis, antioxidant enzymes and lipid peroxidation in soybean seedlings exposed to UV-B radiation and/or Cd. Plant Soil 352:377–387

Li Y, Zhou C, Huang M (2016) Lead tolerance mechanism in *Conyza canadensis*: subcellular distribution, ultrastructure, antioxidative defense system, and phytochelatins. J Plant Res 129(2):251–262

Lichtenthaler HK, Buschmann C(2001). Chlorophylls and carotenoids: measurement and characterization by UV-VIS spectroscopy. Current protocols in food analytical chemistry

Liu J, Mei C, Cai H, Wang M (2015) Relationships between subcellular distribution and translocation and grain accumulation of Pb in different rice cultivars. Water Air Soil Pollut 226:1–9

Ma JF, Ueno D, Zhao F, McGrath SP (2005) Subcellular localisation of Cd and Zn in the leaves of a Cd-hyperaccumulating ecotype of *Thlaspi caerulescens*. Planta 220:731–736

Małecka A, Piechalak A, Morkunas I, Tomaszewska B (2008) Accumulation of lead in root cells of *Pisum sativum*. Acta Physiol Plant 30:629–637

Mingorance MD, Leidi EO, Valdés B, Oliva SR (2012) Evaluation of lead toxicity in Erica andevalensis as an alternative species for revegetation of contaminated soils. Int J Phytoremediat 14:174–185

Mishra S, Srivastava S, Tripathi RD, Kumar R, Seth CS, Gupta DK (2006) Lead detoxification by coontail (*Ceratophyllum demersum* L.) involves induction of phytochelatins and antioxidant system in response to its accumulation. Chemosphere 65:1027–1039

Nishizono H, Ichikawa H, Suziki S, Ishii F (1987) The role of the root cell wall in the heavy metal tolerance of *Athyrium yokoscense*. Plant Soil 101:15–20

Patra J, Lenka M, Panda BB (1994) Tolerance and co-tolerance of the grass *Chloris barbata* Sw. to mercury, cadmium and zinc. New Phytol 128:165–171

Pourrut B, Shahid M, Dumat C, Winterton P, Pinelli E (2011) Lead uptake, toxicity, and detoxification in plants. R Environ Contam Toxico 213:113–136

Qiao X, Zheng Z, Zhang L, Wang J, Shi G, Xu X (2015) Lead tolerance mechanism in sterilized seedlings of *Potamogeton crispus* L.: subcellular distribution, polyamines and proline. Chemosphere 120: 179–187

Salazar MJ, Pignata ML (2014) Lead accumulation in plants grown in polluted soils. Screening of native species for phytoremediation. J Geochem Explor 137:29–36

Sharma P, Dubey RS (2005) Lead toxicity in plants. Braz J Plant Physiol 17:35–52

Srinivasan M, Vikram SS, Favas PJ, Perumal V (2014) Lead heavy metal toxicity induced changes on growth and antioxidative enzymes level in water hyacinths [*Eichhornia crassipes* (Mart.)]. Bot Stud 55:1–11

Sytar O, Kumar A, Latowski D, Kuczynska P, Strzałka K, Prasad M (2013) Heavy metal-induced oxidative damage, defense reactions, and detoxification mechanisms in plants. Acta Physiol Plant 35: 985–999

Tian S, Lu L, Yang X, Webb SM, Du Y, Brown PH (2010) Spatial imaging and speciation of lead in the accumulator plant Sedum alfredii by microscopically focused synchrotron X-ray investigation. Environ Sci Technol 44:5920–5926

Verma S, Dubey RS (2003) Lead toxicity induces lipid peroxidation and alters the activities of antioxidant enzymes in growing rice plants. Plant Sci 164:645–655

Wang S, Zhang J (2006) Blood lead levels in children, China. Environ Res 101:412–418

Wu Z, McGrouther K, Chen D, Wu W, Wang H (2013) Subcellular distribution of metals within *Brassica chinensis* L. in response to elevated lead and chromium stress. J Agr Food Chem 61:4715–4722

Zhao L, Li T, Yu H, Chen G, Zhang X, Zheng Z, Li J (2015) Changes in chemical forms, subcellular distribution, and thiol compounds involved in Pb accumulation and detoxification in *Athyrium war*dii (Hook.). Environ Sci Pollut R, 1–13.

Zhou CF, Wang Y, Li C, Sun R, Yu Y, Zhou D (2013) Subacute toxicity of copper and glyphosate and their interaction to earthworm (*Eisenia fetida*). Environ Pollut 180:71–77

Zhou CF, Wang YJ, Sun RJ, Liu C, Fan GP, Qin WX, Li CC, Zhou DM (2014) Inhibition effect of glyphosate on the acute and subacute toxicity of cadmium to earthworm *Eisenia fetida*. Environ Toxicol Chem 33:2351–2357

Zhou CF, Zhang K, Lin J, Li Y, Chen N, Zou X, Hou X, Ma X (2015) Physiological responses and tolerance mechanisms to cadmium in *Conyza canadensis*. Int J Phytoremediat 17:280–289